Parametrically Driven One-Dimensional Sine-Gordon Equation and Chaos

B. M. Herbst

Department of Applied Mathematics, University of the Orange Free State, Bloemfontein 930, South Africa

W.-H. Steeb

Department of Applied Mathematics and Nonlinear Studies, Rand Afrikaans University, PO Box 524, Johannesburg 2000, South Africa

Z. Naturforsch. **43a**, 727–733 (1988); received January 2, 1988

The chaotic behaviour of the parametrically driven one-dimensional sine-Gordon equation with periodic boundary conditions is studied. The initial condition is $u(x,0) = f(x)$, $u_t(x,0) = 0$ where f is the breather solution of the one-dimensional sine-Gordon equation at $t = 0$. We vary the amplitude of the driving force, the frequency of the driving force and the damping constant. For appropriate values of the driving force, frequency and damping constant chaotic behaviour with respect to the time-evolution of $u(x = \text{fixed}, t)$ can be found. The space structure $u(t = \text{fixed}, x)$ changes with increasing driving force from a zero mode structure to a breather-like structure consisting of a few modes.

1. Introduction

Space-time chaos in non-linear field equations has recently become the focus of much activity. In particular the driven damped sine-Gordon equation [1–7] and the Ginzburg-Landau equation [8–15] have been studied numerically in detail.

In recent studies Mazor et al. [8] and Mazor and Bishop [7] described the destabilisation of the AC-driven damped one-dimensional sine-Gordon equation. They considered the stability of a breather riding on top of a flat background and, in particular, describe the sensitivity of the instability mechanism to the asymptotic phase difference between the breather and the background.

In the present paper we study the parametrically driven sine-Gordon equation

$$u_{tt} + a\,u_t - u_{xx} + [1 + \varepsilon \cos(\Omega t)] \sin u = 0. \quad (1)$$

With $a = 0$ and $\varepsilon = 0$, (1) reduces to the well-known one dimensional sine-Gordon equation

$$u_{tt} - u_{xx} + \sin u = 0. \quad (2)$$

This equation is completely integrable. The second term on the left hand side of (1) describes damping if $a > 0$. We investigate (1) as a function of the driving amplitude ε, the driving frequency Ω and the damping constant a. The initial condition is $u(x,0) = f(x)$ and $u_t(x,0) = 0$, where f is the breather solution of the one-dimensional sine-Gordon equation (2) at $t = 0$.

The space-independent equation

$$u_{tt} + a\,u_t + [1 + \varepsilon \cos(\Omega t)] \sin u = 0 \quad (3)$$

has been studied (mainly numerically) by many authors [16–20]. We summarize the main results in Section 3.

A stability analysis of the breather of the parametrically driven sine-Gordon equation is not trivial and will be attempted elsewhere (see, e.g. the analysis of Mazor and Bishop [7] for the AC-driven damped sine-Gordon equation). In their linearised perturbation analysis they assume that the approximate limit cycle state to be perturbed, is given by $u_0(x,t) = u_B(x,t) + u_v(x,t)$, where u_B is the breather solution and u_v is the steady state solution of the linearised driven damped pendulum. In the present case this ansatz becomes much more complicated since the linearised spatially independent equation is of Mathieu type. However, we do present numerical evidence of a structure of the second instability, not unlike that described by Mazor and Bishop [7].

Reprint requests to Prof. Dr. W.-H. Steeb, Department of Applied Mathematics and Nonlinear Studies, Rand Afrikaans University, PO Box 524, Johannesburg 2000/South Africa.

0932-0784 / 88 / 0800-0727 $ 01.30/0. – Please order a reprint rather than making your own copy.

Dieses Werk wurde im Jahr 2013 vom Verlag Zeitschrift für Naturforschung in Zusammenarbeit mit der Max-Planck-Gesellschaft zur Förderung der Wissenschaften e.V. digitalisiert und unter folgender Lizenz veröffentlicht: Creative Commons Namensnennung-Keine Bearbeitung 3.0 Deutschland Lizenz.

This work has been digitalized and published in 2013 by Verlag Zeitschrift für Naturforschung in cooperation with the Max Planck Society for the Advancement of Science under a Creative Commons Attribution-NoDerivs 3.0 Germany License.

Zum 01.01.2015 ist eine Anpassung der Lizenzbedingungen (Entfall der Creative Commons Lizenzbedingung „Keine Bearbeitung") beabsichtigt, um eine Nachnutzung auch im Rahmen zukünftiger wissenschaftlicher Nutzungsformen zu ermöglichen.

On 01.01.2015 it is planned to change the License Conditions (the removal of the Creative Commons License condition "no derivative works"). This is to allow reuse in the area of future scientific usage.

2. Characterization of Chaos

In our investigation of (1) we study the time evolution of (i) $u(x=0,t)$, (ii) the space structure, i.e. $u(x,t=\text{fixed})$, (iii) the maximal one-dimensional Lyapunov exponent for $u(x=0,t)$, (iv) the frequency spectrum for $u(x=0,t)$ and $u(x,t=\text{fixed})$.

The quantities to characterize chaotic behaviour for ordinary and partial differential equations are the Lyapunov exponents [15, 21–25]. The variational equation (also called linearised equation) of (1) together with (1) must be solved in order to calculate the Lyapunov exponents. The variational equation is determined by

$$\frac{\mathrm{d}}{\mathrm{d}\eta} F(u+\eta y)|_{\eta=0} = 0, \tag{4}$$

where $F(u)$ is given by the left hand side of (1). It follows that

$$y_{tt} + a y_t - y_{xx} + [1 + \varepsilon \cos(\Omega t)] (\cos u)\, y = 0. \tag{5}$$

The linear partial differential equation (5) must be (numerically) solved together with (1).

For the space-independent case, (5) simplifies to

$$y_{tt} + a y_t + [1 + \varepsilon \cos(\Omega t)] (\cos u)\, y = 0. \tag{6}$$

For the space-independent equation (3) the one-dimensional Lyapunov exponents are defined by

$$\lambda = \lim_{T \to \infty} \frac{1}{T} \ln \frac{\mathrm{d}(T)}{\mathrm{d}(0)}, \tag{7}$$

where $\mathrm{d}(t) = [y^2(t) + \dot{y}^2(t)]$ and $y(t)$ denotes the solution of the linearised equation (6). Since (3) is of second order, there are two one-dimensional Lyapunov exponents (i.e., two possible results for the limit (7)) depending on the choice of initial conditions for y and $\dot{y}$. The largest one is obtained for almost any initial condition. This is the one we calculate for the space-independent case.

For partial differential equations we can also define, via the linearised equation (5) and a suitable vector space, Lyapunov exponents (compare [15] and references therein). In the following we restrict ourselfs to the quantity $u(x=0,t)$ and take it as a representative of the spatial behaviour. For this quantity we calculate the maximal one-dimensional Lyapunov exponent.

3. Parametrically Driven Pendulum

The first instability is easily explained in terms of a linearised stability analysis based on the space-independent equation (3). This equation has been studied by many authors [16–20]. McLaughlin [17] studies it numerically with and without damping ($a > 0$ and $a = 0$) and with $\Omega = 2$. In both cases he finds period doubling sequences of bifurcations. Arnedo et al. [18] investigated the stability of the rest solution $u(t) = 0$ and $u_t(t) = 0$ with the aid of the linearised equation where $\Omega = 2$. Koch et al. [19] and Leven et al. [20] give experimental and theoretical evidence for chaotic type nonperiodic solutions of this equation. In order to investigate the stability of the rest state,

$$u(t) = 0, \quad u_t(t) = 0, \quad t \geq 0, \tag{8}$$

we consider the Mathieu equation

$$y_{tt} + a y_t + [1 + \varepsilon \cos(\Omega t)]\, y = 0. \tag{9}$$

The Mathieu equation follows from the linearised equation (6) if we put $u(t) = 0$. It is well-known (see, e.g., Nayfeh and Mook [26]) that the solution of Mathieu's equation grow exponentially for sufficient by large values of ε if

$$\Omega = 2/n, \quad n \geq 1. \tag{10}$$

The principle resonance occurs for $n = 1$. For $\Omega = 2$ it is easy to show [26] that, in addition,

$$\varepsilon > 2a \tag{11}$$

is required for an exponentially growing solution. Consequently, provided condition (11) is satisfied, a small perturbation will grow away from the zero rest state, and numerical experiments show that it evolves into a limit cycle of period 2π. If $a = 0.1$, numerical calculations show that this situation will persist until $\varepsilon \approx 1$, although period doubling sequences of bifurcations may take place (see, e.g., McLaughlin [17]). A further fractional increase in ε causes the solution to become chaotic. In Fig. 1 we give the approximate transition line to chaos in the (ε, Ω)-plane, resulting from a numerical study of (1) with $a = 0$. The initial values are $u(0) = 5.48$ and $u_t(0) = 0$. With increasing $\Omega (\Omega > 2)$ the quantity ε_{cr} becomes larger. The same holds for decreasing $\Omega (\Omega < 2)$. Within the chaotic region one finds periodic windows.

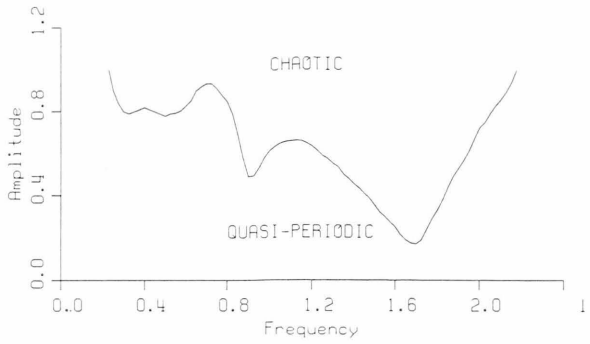

Fig. 1. The transition line to chaos of the parametrically driven pendulum with $a = 0$ and $u(0) = 5.48$ and $u_t(0) = 0$.

4. Numerical Method

We now proceed to our numerical studies of (1). The initial condition which we consider is $u(x, 0) = f(x)$, $u_t(x, 0) = 0$, where

$$f(x) = 4 \arctan \{c^{-1}(1 - c^2)^{1/2} \operatorname{sech}[1 - c^2)^{1/2} x]\} \quad (12)$$

with $c = 0.2$. Thus the function f is the breather solution at $t = 0$ of the one-dimensional sine-Gordon equation (2). In addition, the periodic boundary condition $u(x + L, t) = u(x, t)$ is imposed with $L = 32$.

The Fourier pseudospectral method [27] is used to discretise the space variables. Let $\{g_j\}$, $-\infty < j < \infty$, be a periodic sequence of complex numbers such that $g_{j+N} = g_j$. Furthermore, assume that the sequence is derived from a periodic complex function, $g(x + L) = g(x)$, such that $g_j = g(x_j)$, where $x_j = hj$ and $h = L/N$. We define the discrete Fourier transform, $\mathcal{F}$, of the sequence by

$$\hat{g}_n = \mathcal{F}_n\{g_j\} = \sum_{j=0}^{N-1} g_j \exp(-i\mu_n x_j), \quad (13)$$

where $\mu_n = 2\pi n/L$. The discrete inverse transform is then given by

$$g_j = \mathcal{F}_j^{-1}\{\hat{g}_n\} = \frac{1}{N} \sum_{n=0}^{N-1} \hat{g}_n \exp(i\mu_n x_j). \quad (14)$$

The spatial variables of the parametrically driven sine-Gordon equation is now discretized in the following way:

$$\ddot{U}_j + a\dot{U}_j + \mathcal{F}_j^{-1}\{\mu_n^2 \mathcal{F}_n\{U_k\}\} + [1 + \varepsilon \cos(\Omega t)] \sin U_j = 0, \quad (15)$$

where $j = 0, 1, \ldots, N-1$. We emphasize that periodic boundary conditions, $U_{j+N} = U_j$, are imposed. Throughout the calculation $L = 32$ and $N = 64$ are used.

The semi-disccrete system (15) is integrated in time by the Runge-Kutta Merson scheme, DO2BBF, with accuracy specified as 10^{-4}, and the numerical experiments are performed in double precision using the RM-Fortran compiler on the Intel 80286/7 processors.

Finally, we note the superiority of the pseudospectral method over second and fourth order finite differences [28]. In some applications pseudospectral methods may require as little as a quarter the number of grid points as compared with fourth order finite differences and as little as one-sixteenth the number of grid points as second order finite differences.

5. Numerical Results

The parametrically driven sine-Gordon equation contains three free parameters, a, ε and Ω. We therefore perform three sets of numerical studies. In each set two of the parameters are fixed and the consequence of varying the third is examined. In this way we are able to cover a reasonable part of the parameter space. In the experiment we use the initial condition, $u(x, 0) = f = (x)$, $u_t(x, 0) = 0$ where f is the breather solution (12) of the one-dimensional sine-Gordon equation at $t = 0$.

In some of the studies we let f take on random values between zero and 0.1. In this way we can test the stability of the zero solution numerically and can also obtain an indication of how the asymptotic state depends on the choice of the initial condition. We refer to this initial condition as random initial conditions to distinguish it from the previous breather initial condition.

When we refer to the temporal behaviour of the system, we mean the temporal behaviour of the solution $u(x, t)$ at $x = 0$, which we take as representative of the spatial behaviour. However, the evolution of the spatial structure is also monitored and will be discussed when appropriate.

We start the description of the numerical experiments by keeping a and Ω fixed and varing ε. In the first set of experiments we choose $a = 0.1$ and $\Omega = 1.5$. In this case the situation is fairly simple. For values of ε, typically $0 < \varepsilon < 0.922$, the damping term dominates and the solution quickly, after about $t \approx 100$, settles down to the zero solution $u(x, t) = 0$ which, as

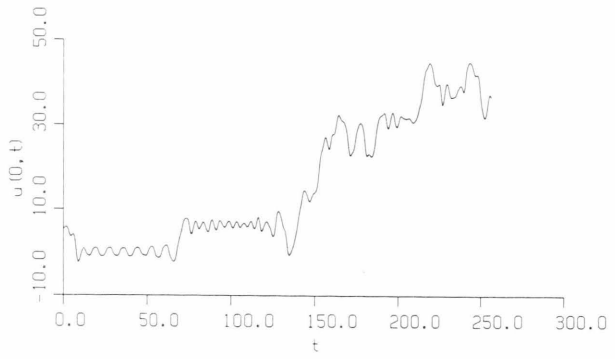

Fig. 2. Time evolution of $u(x=0,t)$ for $\varepsilon = 0.923$, $\Omega = 1.5$ and $a = 0.1$.

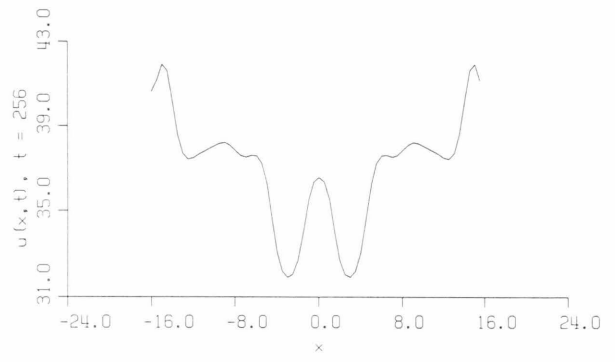

Fig. 3. Spatial structure $u(x, t=256)$ for $\varepsilon = 0.923$, $\Omega = 1.5$ and $a = 0.1$.

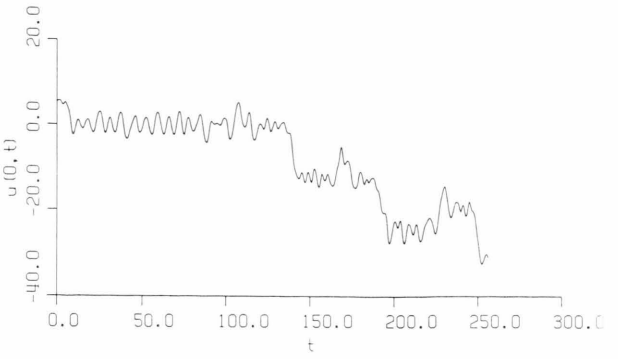

Fig. 4. Time evolution $u(x=0,t)$ for $\varepsilon = 0.932$, $\Omega = 2.0$ and $a = 0.1$.

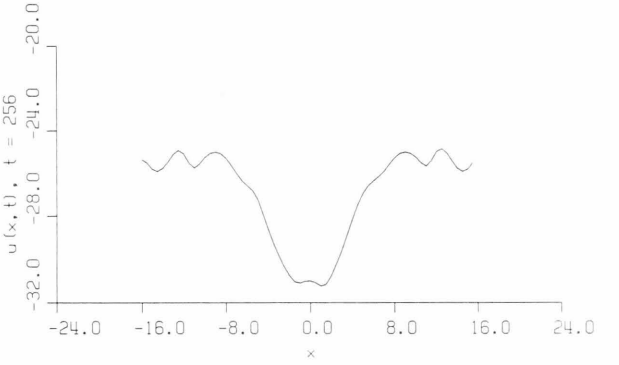

Fig. 5. Spatial structure $u(x, t=256)$ for $\varepsilon = 0.932$, $\Omega = 2.0$ and $a = 0.1$.

we recall, is a fixed point of the parametrically driven sine-Gordon equation. At $\varepsilon = 0.923$, there is a bifurcation in the solution. The time evolution has become chaotic, showing up as an "escaping" solution. This is due to the fact that the potential is given by $U(x) = -\cos(x)$. At the same time the spatial structure changes to one consisting of a few lower Fourier modes. Figure 2 shows the time evolution of $u(x=0,t)$ for this value. In Fig. 3 we give the spatial structure for this value at $t = 256$. We stress that the change from the zero solution to the chaotic solution is sudden; we have not been able to identify any transitional state (such as a Feigenbaum sequence) between the two.

The choice $\Omega = 2$ is special since it corresponds to one of the well-known unstable values of Mathieu's equation. In fact, we mentioned earlier that the zero solution of the parametrically driven one-dimensional sine-Gordon equation, for this value of Ω becomes unstable whenever $\varepsilon > 2$. In this case, it means that the zero solution becomes unstable for $\varepsilon > 0.2$. For $\varepsilon < 0.2$ the solution settles down to the zero solution. For $\varepsilon > 0.2$ the solution looses its spatial structure and becomes the extended flat, or μ_0 mode in space where $\mu_n = 2\pi n/L$, where L is the spatial period, namely 32 in our numerical studies. This zero spatial mode oscillates in time with a period $T = 1/(2\pi)$, i.e., twice that of the driver. This situation persists up to about $\varepsilon = 0.931$, and for $\varepsilon = 0.932$ the time evolution of $u(x=0,t)$ has become chaotic. We also observe a difference in the spatial structure of the solution which coincides with the change in the temporal behaviour. The spatial dependence changes from the zero mode structure to one consisting of a few frequencies. Again we are unable to find any transitional state, such as a period doubling, etc. Figure 4 shows the time evolution of $u(x=0,t)$ for $\varepsilon = 0.932$, and Fig. 5 reveals the spatial structure for this value at $t = 256$.

The aforementioned results we obtained from the breather initial condition. However, we do not find any qualitative difference using a random initial con-

dition. The only noticeable difference is that the bifurcation from the oscillation to the chaotic solution occurs at a slightly different value of ε. This is probably not significant, since the transition also occurs at a different value of ε if, for instance, the accuracy of the time integrator is changed.

We now fix the values of ε and a at $\varepsilon = 1.0$ and $a = 0.1$ and vary Ω. In this case we find chaos in the temporal behaviour, for values of Ω roughly between 1 and 2. For small and large values of Ω the solution decays to the zero solution. The zero solution becomes unstable if Ω is increased through 0.55 or decreased through 6. Changing the value of Ω between these two values results in a complicated series of bifurcations.

If we use the breather initial condition and increase the value of Ω through 0.55 we find that the spatial structures of the asymptotic state changes from the zero mode to a breather-like structure consisting of several low-order modes. For $\Omega = 0.6$ this breather-like solution is quasi-period in time, oscillating at three distinct frequencies of the form $\cos(\mu t)$ with $\mu = 0.295, 0.896$ and 1.497. Hence, the temporal oscillations consist of a fundamental mode, $\mu = 0.896$, and two side modes. Our numerical studies indicate that the energy in the random initial conditions is not sufficient to excite the breather-like structure in space. Instead, we again find the extended zero mode which, nervertheless, oscillates at exactly the same frequencies as the breather.

A further increase in the value of Ω, again using the breather initial condition, shows a sudden transition to chaotic temporal behaviour for a small window in the region of $\Omega = 0.8$, without any significant change in the spatial structure. However, for slightly higher values of Ω the spatial structure bifurcates and takes the form of a single higher Fourier mode. Simultaneously, the temporal oscillation locks onto a single frequency, for example, for $\Omega = 1.22$ we find an asymptotic state approximately of the form

$$u(x, t) = \cos(\pi x/4)\cos(1.215\, t). \tag{16}$$

Clearly the temporal oscillation has locked onto the driver frequency.

As Ω is increased it becomes increasingly difficult to study the transition numerically. We find that the slightest change in the numerical scheme may alter the qualitative behaviour of the solution. Also, the solution becomes extremely sensitive to rounding errors in the sense that the symmetric spatial structure resulting from the breather initial condition is destroyed, even after times as short as $t = 512$, despite the symmetry of the problem. For Ω in the vicinity of 1.35 the temporal behaviour of $u(x = 0, t)$ becomes chaotic. In this case the chaos manifests itselve in the form of an escaping solution. This coincides with another change in the spatial structure. Now the spatial structure again consists of a few lower Fourier modes. Again we have not been able to identify any transition from the steady oscillation to chaos. In Fig. 6 the time-evolution of $u(x = 0, t)$ is depicted for $\Omega = 1.35$, and Fig. 7 shows the spatial structure at $t = 256$. Figure 8 shows the power spectrum of the spatial structure.

A further increase in Ω to about 3 gives a return to the steady oscillations in time. Also the spatial structure again assumes the form of a single higher frequency in space. The situation persists for values of Ω up to about 6. For instance, for $\Omega = 5.5$ we find that the asymptotic state assumes the approximate form, $\cos(2.55\, x)\cos(2.75\, t)$. Hence, a subharmonic is formed with as period twice that of the driver. Using the random initial conditions at these same parameter values gives exactly the same asymptotic state, indicating a large basin of attraction. In Fig. 9 the time-evolution of $u(x = 0, t)$ is depicted for $\Omega = 5.5$, and Fig. 10 shows the spatial structure at $t = 256$. For the time-evolution we find a transient region. Figure 11 shows the power spectrum of the spatial structure. Figure 12 presents the time-evolution with random initial conditions, and Fig. 13 contains the spatial structure at $t = 256$.

In the previous calculations a rather large damping constant, $a = 0.1$, was used, which required large values of ε in order to destabilise the system. Now we fix $\varepsilon = 0.7$ and $\Omega = 0.9$ and investigate the changes caused by varying the damping constant a. As can be expected, for large values of a, e.g., $a = 0.5$, the asymptotic state is simply the zero solution. If the value of a is decreased, e.g. $a = 0.1$, we find that the asymptotic state is a steady oscillation in time with a main frequency of 0.908, i.e., the temporal oscillation is locked onto that of the driver. Simultaneously, the spatial structure changes from the extended zero mode to a breather-like structure. Unlike the previous case, where we encountered a quasi-periodic breather-like structure, this one oscillates at a single frequency. Again we note that the random initial condition does not contain enough energy to excite the breather. We find that the asymptotic state, for random initial conditions, is the zero solution. A further decrease in the

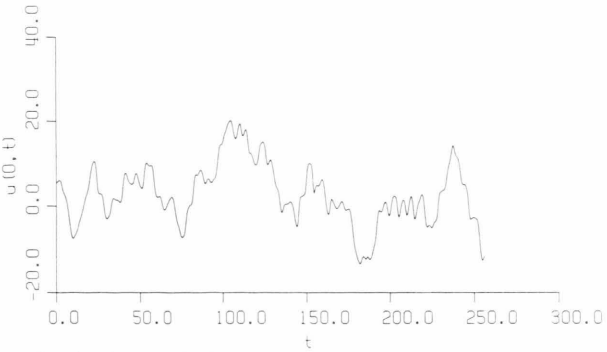

Fig. 6. Time evolution of $u(x = 0, t)$ for $\varepsilon = 1.0$, $\Omega = 1.35$ and $a = 0.1$.

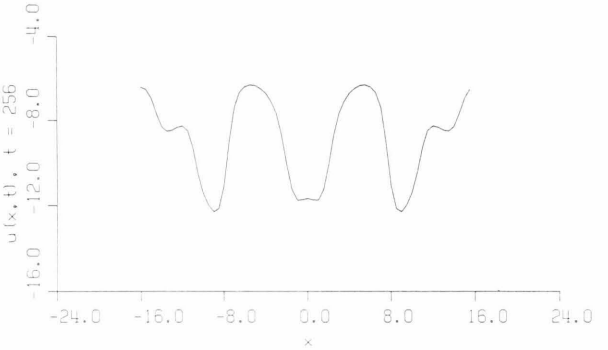

Fig. 7. Spatial structure $u(x, t = 256)$ for $\varepsilon = 1.0$, $\Omega = 1.35$ and $a = 0.1$.

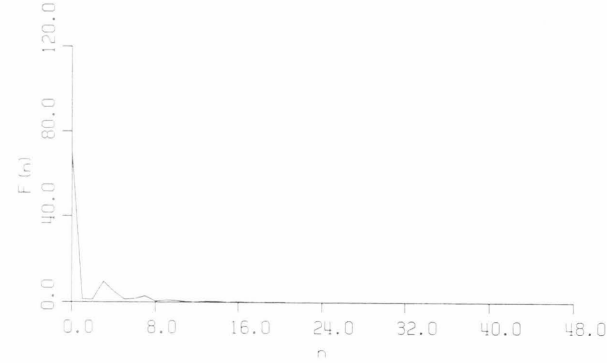

Fig. 8. Power spectrum of the spatial structure $u(x, t = 256)$ for $\varepsilon = 1.0$, $\Omega = 1.35$ and $a = 0.1$.

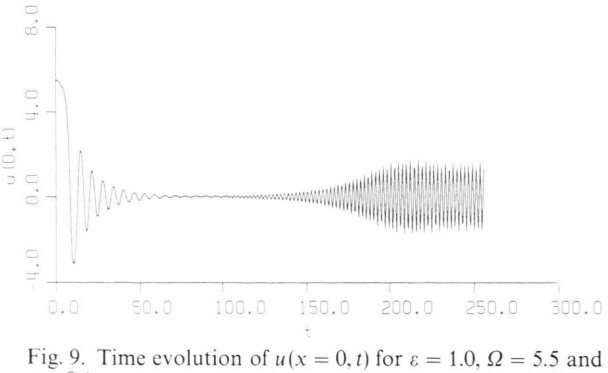

Fig. 9. Time evolution of $u(x = 0, t)$ for $\varepsilon = 1.0$, $\Omega = 5.5$ and $a = 0.1$.

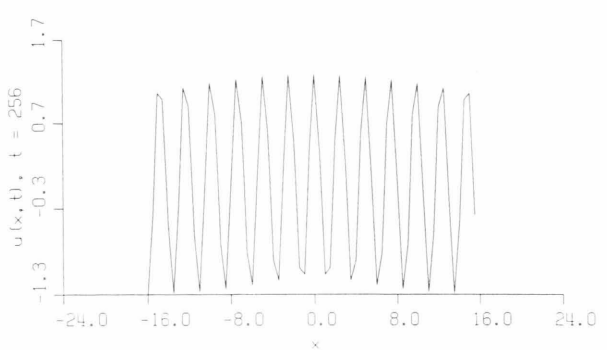

Fig. 10. Spatial structure $u(x, t = 256)$ for $\varepsilon = 1.0$, $\Omega = 5.5$ and $a = 0.1$.

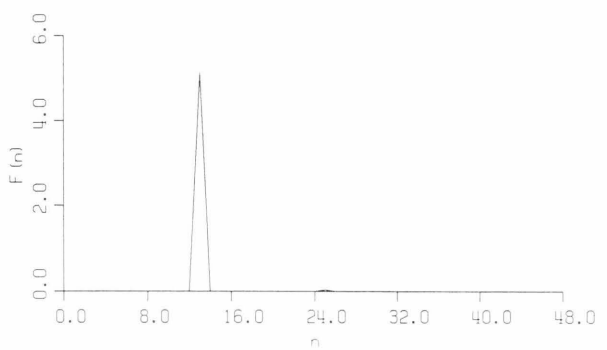

Fig. 11. Power spectrum of $u(x, t = 256)$ for $\varepsilon = 1.0$, $\Omega = 5.5$ and $a = 0.1$.

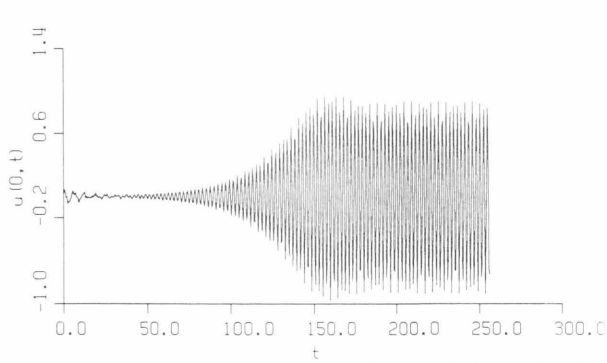

Fig. 12. Time evolution of $u(x = 0, t)$ for $\varepsilon = 1.0$, $\Omega = 5.5$ and $a = 0.1$ with random initial conditions.

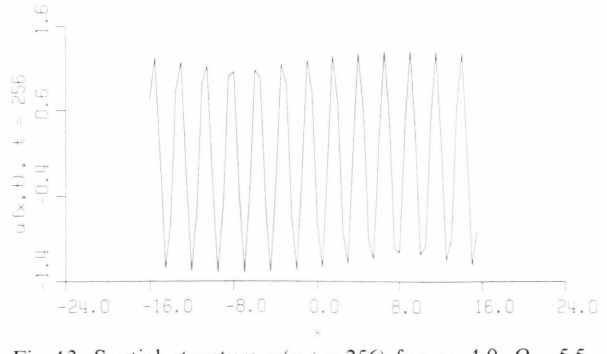

Fig. 13. Spatial structure $u(x, t = 256)$ for $\varepsilon = 1.0$, $\Omega = 5.5$ and $a = 0.1$ with random initial conditions.

value of a to $a = 0.07$ or $a = 0.06$ causes side modes to appear in the temporal oscillation while retaining the breather like spatial structure. A further decrease in a leads to further modes appearing until at $a = 0.0275$ a broad Fourier spectrum, typical of chaos, appears. Therefore, for these parameter values there are clear indications that there is a definite road to chaos. We also observe that the chaos does not have the escaping character of the chaos of the previous studies. Only for very small values of a do we find the first signs of an escaping solution.

6. Conclusions

We have studied the one-dimensional parametrically driven sine-Gordon equation. Whereas we find chaotic behaviour in the temporal evolution, i.e. the evolution of $u(x = 0, t)$ for appropiate values of ε, Ω and a, the spatial pattern does not give complex behaviour. However, in all cases chaotic temporal behaviour is accompanied by the spatial structure consisting of a few lower Fourier modes. This structure is obtained from completely different initial conditions and does not appear to depend on the initial state in situations where temporal chaos is obtained. We also encounter very complicated series of bifurcations in the spatial structure, in particular when ε and a are kept constant and Ω is varied. This is not well understood. However, the particularly simple spatial structures sometimes encountered, as in Fig. 10 and 13, open the possibility of further theoretical investigations which are currently undertaken.

[1] J. C. Eilbeck, P. S. Lomdahl, and A. C. Newell, Phys. Lett. **87 A,** 1 (1981).
[2] A. R. Bishop, K. Fesser, P. S. Lomdahl, W. C. Kerr, M. B. Williams, and S. E. Trullinger, Phys. Rev. Lett. **50,** 1095 (1983).
[3] A. R. Bishop, K. Fesser, P. S. Lomdahl, and S. E. Trullinger, Physica **7 D,** 259 (1983).
[4] A. R. Bishop, M. G. Forest, D. W. McLaughlin, and E. A. Overman II, Physica **23 D,** 293 (1986).
[5] A. R. Bishop and P. S. Lomdahl, Physica **18 D,** 54 (1986).
[6] A. Mazor, A. R. Bishop, and D. W. McLaughlin, Phys. Lett. **119 A,** 273 (1986).
[7] A. Mazor and A. R. Bishop, Physica **27 D,** 269 (1987).
[8] H. T. Moon, P. H. Huerre, and L. G. Redekopp, Phys. Rev. Lett. **49,** 458 (1982).
[9] E. A. Caponi, P. G. Saffman, and H. C. Yuen, Phys. Fluids **25,** 2159 (1982).
[10] K. Nozaki and N. Bekki, Phys. Rev. Lett. **51,** 2171 (1983).
[11] I. S. Aranson, A. V. Gaponov-Grekov, M. I. Rabinovich, and I. P. Starobinets, Sov. Phys. JETP **63,** 1000 (1986).
[12] K. Nozaki and N. Bekki, Physica **21 D,** 381 (1986).
[13] A. Aceves, H. Adachihara, C. Jones, J. C. Lerman, D. W. McLaughlin, J. V. Moloney, and A. C. Newell, Physica **18 D,** 85 (1985).
[14] P. Holmes, Physica **23 D,** 293 (1986).
[15] C. R. Doering, J. D. Gibbon, D. D. Holm, and B. Nicolaenko, Phys. Rev. Lett. **59,** 2911 (1987).
[16] R. W. Leven and B. P. Koch, Phys. Lett. **86 A,** 71 (1981).
[17] J. B. McLaughlin, J. Stat. Phys. **24,** 375 (1981).
[18] A. Arnedo, P. Coullet, C. Tresser, A. Libchaber, J. Maurer, and D. d'Humieres, Physica **6 D,** 385 (1983).
[19] B. P. Koch, R. W. Leven, B. Pompe, and C. Wilke, Phys. Lett. **96 A,** 219 (1983).
[20] R. W. Leven, B. P. Koch, B. Pompe and C. Wilke, Physica **16 D,** 371 (1985).
[21] J. Wright, Phys. Rev. **29 A,** 2923 (1984).
[22] A. Wolf, J. B. Swift, H. L. Swinney, and J. A. Vastano, Physica **16 D,** 285 (1985).
[23] J. M. Greene and Jin-Soo Kim, Physica **24 D,** 213 (1987).
[24] M. Sano and Y. Sawada, Phys. Rev. Lett. **55,** 1082 (1985).
[25] W.-H. Steeb and J. A. Louw, Chaos and Quantum Chaos, World Scientific, Singapore 1986.
[26] A. H. Nayfeh and D. T. Mook, Nonlinear Oscillations, J. Wiley, New York 1979.
[27] D. Gottlieb, M. Y. Hussaini, and S. A. Orszag, "Spectral Methods for Partial Differential Equations, edit. by R. G. Voigt et al", in "," SIAM, Philadelphia, 1984.
[28] B. Fornberg, Geophysics **52,** 483 (1987).